Letters in Applied NanoBioScience
Open-Access Journal (ISSN: 2284-6808)

Article
Volume 15, Issue 3, 2026, 88
https://doi.org/10.33263/LIANBS153.088

AQbD-Based Robust and Green HPTLC Method for Simultaneous Estimation of Memantine and Galantamine in Smart Long-Acting Injectable Formulation (SLAIF)

Prachi Rabari [1], Hardik Rana [2,*], Devang Tandel [3], Vaishali Thakkar [4]

[1] Research scholar, Gujarat Technological University, Ahmedabad, Gujarat, India
[2] Department of Pharmaceutics, Anand Pharmacy College, Anand, Gujarat, India
[3] Department of Quality Assurance, Anand Pharmacy College, Anand, Gujarat, India
[4] Department of Pharmaceutics, Anand Pharmacy College, Anand, Gujarat, India
* Correspondence: hardikrana1439@gmail.com;

Received: 23.06.2025; Accepted: 20.02.2026; Published: 01.07.2026

Abstract: A greener analytical quality by design (AQbD)-based HPTLC method was developed for the simultaneous quantification of Memantine HCl (MH) and Galantamine HBr (GH) in a smart long-acting injectable formulation. The MH–GH combination offers synergistic cognitive benefits, necessitating a reliable analytical approach for their co-estimation. Chromatographic separation was achieved using chloroform–cyclohexane–methanol–ammonia (5:3:2:0.2, v/v/v/v) as the mobile phase. AQbD principles were implemented by defining the Analytical Target Profile and Critical Analytical Attributes. Robustness was evaluated using a 2^{4-1} fractional factorial design. Distinct and well-resolved bands were obtained at Rf values of 0.56 for GH and 0.28 for MH. The method showed excellent linearity (1500–4000 ng/band; $r^2 > 0.998$), precision (RSD < 2%), and accuracy (recoveries 99–101%). The limits of detection and quantification were 63 and 192 ng/band for GH and 88 and 267 ng/band for MH. High greenness scores (BAGI = 80, Analytical Eco-Scale =74) confirmed its eco-friendly nature. The developed AQbD-based HPTLC method is robust, specific, sensitive, and environmentally sustainable, and can be effectively applied for the quantitative analysis of MH and GH in long-acting injectable formulations.

Keywords: AQbD; BAGI; complex GAPI; memantine HCl; galantamine HBr; fractional factorial design.

1. Introduction

The world is moving toward developing environmentally friendly methods for designing, formulating, and assessing the formulated product. The main goal is to minimize waste, avoid the use of harmful substances, and reduce energy consumption without affecting the process efficiency. The method should also be user-friendly [1]. The environmental friendliness of the method was assessed using several tools [2]. The Blue Applicability Grade Index (BAGI), the Green Analytical Procedure Index (COMPLEX GAPI), and the Analytical Eco-Scale are examined in the current research to evaluate the greenness of the technique.

In the current research, the chosen molecules are GH and MH, which are coming under the anti-Alzheimer category[3,4]. Both molecules are chosen as they are the most prescribed

medications in the management of Alzheimer's disease (AD). AD is prevalent in the geriatric population instead of adults. The condition of AD worsens as age increases. Right now, 40 million people are suffering from AD, as per the report [5]. There is no proper treatment presently for AD, and only symptomatic treatment is available [6]. MH is coming under the NMDA receptor antagonist, and GH is coming under the cholinesterase inhibitors [7]. The combination of GH and MH was selected due to their diverse actions on the treatment of AD [8].

MH, an extra synaptic NMDAR antagonist, is presently utilized alongside acetylcholinesterase inhibitors for the management of AD. MH inhibits the activation of NMDAR without affecting the routine functionality of the synapse [9–11]. GH is a reversible, competitive acetylcholinesterase inhibitor. It competitively and reversibly inhibits the acetylcholine esterase in the CNS. By blocking the cessation of ACh, it enhances ACh levels in the synaptic cleft [12–14]. When combined with an NMDA receptor antagonist, it gives an additive or synergistic effect [15–17]. The chemical structure of both drugs is shown in Figure 1.

Several chromatographic techniques, such as HPLC, HPTLC, and LC-MS, have been reported for the estimation of GH or MH alone [18–20]. However, to date, no HPTLC method has been developed for the simultaneous quantification of MH and GH in combination. Hence, the current study aims to fill this research gap by developing and validating an HPTLC method for the concurrent estimation of GH and MH in combination. HPTLC is widely preferred for drug analysis due to its cost-effectiveness, rapid analysis time, minimal solvent consumption, and reduced sample preparation requirements. Moreover, it facilitates automated sample application and plate scanning, enhancing analytical efficiency [21,22].

Additionally, the method was developed by applying the AQbD methodology to reduce organic flush and utilize the least energy. AQbD provides a methodical, reliable approach to creating analytical procedures that encompass every phase of a product's lifecycle. Identification of Analytical target profile (ATP), critical analytical attributes (CAAs), critical method attributes (CMAs), risk examination, design space, optimization of processing conditions, and control strategy are the six components of AQbD [23–25].

Parameters, including linearity, accuracy, precision, resilience, and analysis of the developed formulation, were used to validate the method. A fractional factorial design (FFD) was chosen among the different statistical designs for nonlinear response prediction. Owing to the non-availability of a chromophoric group in the structure of MH, Eosin Y (EY) dye was chosen as a derivatizing agent based on a literature survey. The use of EY improves the detection power of the MH and is also cost-effective [18,26,27].

The current study aims to develop a green, robust, precise, and sensitive technique for the quantification of MH and GH in a developed smart long-acting injectable formulation (SLAIF) using advanced analytical and statistical design. Additionally, three greenness metric tools like BAGI, COMPLEX GAPI, and analytical eco-scale were employed for the assessment of the method's greenness.

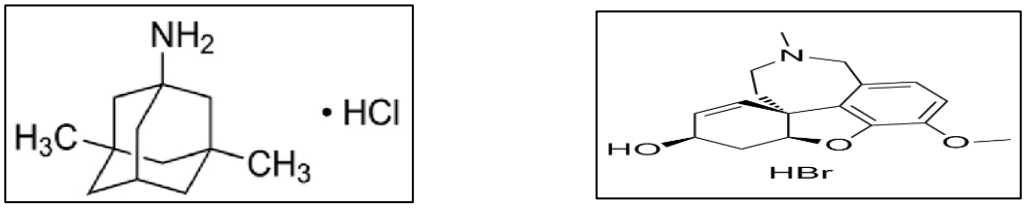

(a) **(b)**

Figure 1. Structure of **(a)** MH; **(b)** GH.

2. Materials and Methods

2.1. Materials.

MH and GH were kindly provided as a gift sample (purity-99.99%) from ZCL Chemicals Ltd, India. EY dye was provided by Chemdyes Corporation India (purity-99 %). The supplier of all other HPLC-grade chemicals and solvents was Merck. Specialties Pvt. Ltd., India.

2.2. Instrumentation.

Precoated silica gel 60 F254 aluminium plates with pre-defined dimensions (10 x10cm, 100 µm thickness) from Merck, Germany, Sample applicator - Linomat 5, Hamilton syringe (100 µL), TLC scanner-4, Flat bottom and twin through chamber' (10 x 10 cm), UV area having dual wavelength UV lamp, WinCATS version 1.4.6 software from Camag, Switzerland, Analytical balance from Shimadzu, Germany and ultrasonic bath from ultrasonic cleaner, Mumbai.

2.3. Preparation of GH and MH stock solution.

A 1000 µg/mL solution of GH and MH was prepared by dissolving 10mg of GH and MH separately in 10 mL of methanol.

2.4. EY Dye preparation for the derivatization process.

The EY dye was chosen for the study after preliminary trials and analytical expertise [28]. After taking preliminary trials, 0.05% of the EY dye was optimized for the detection of MH. A sufficient quantity of the EY dye was dispersed in 80:20 %v/v ratio of ethanol: water. The prepared dye solution was sprayed over the TLC plate, and air-dried after derivatization.

2.5. Separation technique.

Standard and sample solutions were added to the HPTLC plates as bands. The band was 6mm long and located 10mm from the bottom and from the edges. A 'Camag Linomat V sample applicator' was utilized for the application of the band. The pre-defined HPTLC plates were used for the current study. The chromatographic run had a distance of 80 mm, and the mobile phase was composed of chloroform: cyclohexane: methanol: ammonia (5:3:2:0.2 %v/v/v/v). The development compartment was allowed to equilibrate with the mobile phase for 20 min before the commencement of the trial. The bottom-up approach was utilized to lift the phase to 8cm. The plates were dried at 27±0.5°C. The observation was reported at 230 nm for GH (before derivatization) and 547nm for MH (after derivatization), accomplishing a densitometric scanning process.

2.6. Implementation of AQbD methodology.

2.6.1. Identification of ATP, CMA, and risk assessment parameters.

The first important stage in developing an AQbD analysis technique is to precisely define the ATP to identify its key objectives and potential outcomes [29]. According to ICH Q8 (R2), the Analytical Target Profile (ATP) defines the method requirements and measurable

criteria essential for method development, specifying what to measure (e.g., impurity levels and acceptance criteria) and the required performance characteristics, such as robustness, sensitivity, and precision [25,30]. In the AQbD framework, Critical Method Attributes (CMAs) influence the Critical Analytical Attributes (CAAs) that determine HPTLC method performance. Based on literature and preliminary studies, the relevant method attributes were evaluated, and the most influential CAAs were identified as key performance indicators [31]. Following ICH Q8 and Q9 guidelines, a risk-based approach was adopted to assess the robustness of the developed method. CAAs and CMAs were correlated through risk assessment to identify attributes influencing the ATP. An Ishikawa diagram developed through brainstorming summarized potential factors affecting CAAs, highlighting the most critical ones based on prior studies. A risk assessment matrix (RAM) was then used to pinpoint variables with the highest impact on CAAs, which were further correlated using a 2^{4-1} fractional factorial design (FFD) [32,33].

2.7. Method validation.

The analytical technique was validated in accordance with the recent regulatory ICH guideline. The technique was validated for the regulatory validation parameter. The robustness of the method was assessed by the application of a systematic and scientific approach [34].

2.7.1. DoE-mediated robustness.

The ICH recommendations were followed while assessing the robustness of an analytical method. Robustness was investigated using the 2^{4-1} fractional factorial design, using Design Expert 13 version. Fractional factorial designs are a fraction of the full factorial experiment. A fractional factorial design was preferred over a Plackett–Burman design because it allows for the evaluation of both main and interaction effects with fewer experimental runs. This provides a better understanding of factor interplay and enhances the reliability of analytical method optimization. Four CMAs were selected for this study based on prior experience, chromatographic instinct, and the significance of variables found during trial runs i.e., Volume of methanol (A – 1.8 to 2.2 mL) and Volume of chloroform (B- 4.8 to 5.2 mL) in mobile phase component, Chamber saturation time (C- 18 to 22 min), and Solvent front (D- 75 to 85 mm). As a critical quality attribute, Y1 = Rf of GH (Desired range: 0.51-0.61)and Y2 = Rf of MH (Desired range: 0.25-0.35) were chosen. The four variables, along with their high and low levels, were listed above.

Table 1. Design matrix with their responses of FFD.

Run	A (mL)	B (mL)	C (min.)	D (mm)	Y_1	Y_2
1	2.2	5.2	18	75	0.56	0.33
2	2.2	4.8	22	75	0.54	0.29
3	1.8	4.8	22	85	0.52	0.25
4	1.8	5.2	18	85	0.63	0.35
5	2.2	5.2	22	85	0.65	0.37
6	1.8	5.2	22	75	0.53	0.27
7	1.8	4.8	18	75	0.51	0.27
8	2.2	4.8	18	85	0.60	0.32

The chosen variables were varied at different levels with varied combinations, and a design matrix was generated as shown in Table 1. The trials were performed as per the design matrix, and responses were evaluated for each trial. Analysis of variance and multiple linear regression analysis were used to evaluate each variable's impact on the selected responses. P-value and correlation coefficient of each response were measured. Based on the value of the p-value and

correlation coefficient, the influence of the variable on the response was estimated. P-value more than 0.05 required for insignificant change. Generally, a value of the correlation coefficient less than 10% is preferred. The polynomial equation was generated to comprehend the association between dependent and independent factors. Pareto charts, perturbation maps, and two-dimensional and three-dimensional graphs were plotted to understand the relationship systematically.

2.7.2. Calibration curve and linearity.

To ascertain the consistent correlation between peak area and GH/MH concentration, five replicate measurements were taken for GH and MH within the concentration range of 1500–4000 ng/band. Regression analysis was employed for the standard curve of GH and MH, utilizing MS Excel. An HPTLC plate was spotted with varying quantities of stock solution (1.5, 2.0, 2.5, 3.0, 3.5, and 4.0 µL) to achieve concentrations of 1500, 2000, 2500, 3000, 3500, and 4000 ng/band, respectively. Linear least-squares regression was utilized to analyze the peak area versus drug concentration data.

2.7.3. Limit of detection (LoD) and limit of quantitation (LoQ).

The method's LoD and LoQ were determined from the standard deviation of the response and the slope of the GH and MH calibration curves, following ICH guidelines, as shown in Equations 1 and 2.

$$LoD = 3.3\ \frac{\sigma}{S} \qquad (1)$$

$$LoQ = 10\ \frac{\sigma}{S} \qquad (2)$$

Where "σ" is the standard deviation of the response and "S" is the slope of the standard plot.

2.7.4. Precision.

The developed technique's precision was assessed by executing multiple measurements of the sample to evaluate repeatability, intra- and inter-day precision. Three varied concentrations (2000ng, 3000ng, and 4000ng) of GH and MH were carried out under the same experimental conditions. The study was performed thrice on a single day and a single time for three consecutive days.

2.7.5. Accuracy.

Recovery measurements were performed to verify the technique's accuracy by adding 1600 ng/band of GH and MH to samples at 50, 100, and 150% levels. The samples were then analyzed in triplicate using the suggested approach.

2.7.6. Specificity.

The spectra of developed SLAIF were compared to reference drug spectra to measure the specificity. Additionally, the peak purity of GH and MH was estimated by relating observations at three points: initiation, apex, and end of the peak. A standard densitogram was used to measure the Rf of GH and MH in the developed smart formulation to assess any excipient influence.

2.7.7. Analysis of developed SLAIF.

The SLAIF preparation involves sequential steps. First, in the internal polymer phase, PLGA is dissolved in a suitable organic solvent, and the drug is incorporated by agitation until

a clear solution forms. Simultaneously, the external phase is prepared by mixing oil with a surfactant and a co-surfactant to ensure homogeneity. The two phases are then combined via sonication or homogenization, forming a stable dispersion of bio-nano globules. Finally, the injectable solution is introduced into a phosphate buffer (pH 7.4), triggering bio-nano particle formation for controlled drug delivery. GH and MH concentrations in SLAIF were evaluated by taking an equivalent of 5 mg of GH and MH, which were solubilized in 5 mL of pH 7.4 Phosphate buffer, and the mixture was sonicated for 10 minutes to get 1000 µg/mL GH and MH. Whatman filter paper no. 42, which had been formerly saturated in methanol, was then used to filter the mixture. The HPTLC plate was spotted with 3 µl of the filtered solution to get a final concentration of 3000 ng/band, followed by scanning and development.

2.7.8. Greenness appraisal.

Developing a green quantification method is essential in the current era. Green Analytical Chemistry (GAC) aims to optimize analytical procedures by minimizing energy consumption, hazardous waste, and unsafe reagents while ensuring analyst safety. To assess the method's sustainability, greenness was evaluated using three tools: BAGI, Complex GAPI, and the Analytical Eco-Scale [35–38]. BAGI, a novel metric system, evaluates the practicality of analytical methods based on ten key parameters. It generates an asteroid pictogram with color gradients indicating compliance—dark blue (high), blue (medium), light blue (low), and white (none). The central score, ranging from 25 to 100, reflects overall method performance, with 25 indicating poor applicability and 100 indicating excellent applicability. A minimum score of 60 indicates acceptable feasibility [2,39]. The COMPLEX GAPI is the second evaluation tool, assessing factors such as energy use, solvent and reagent consumption, sample preparation, and analytical technique. It aids in identifying opportunities to minimize environmental impact. The method is depicted through a 15-segment colored pictogram—green indicates low, yellow moderate, and red high environmental impact [1,40,41]. The Analytical Eco-Scale, the third assessment tool, provides a comprehensive evaluation of method greenness using a penalty point system. Hazardous chemicals are assigned penalty points—zero for none, one for minor, and two for major hazards. Energy consumption is also scored according to Raynie and Driver's guidelines, with techniques such as NMR, GC–MS, and LC–MS (>2.5 h) being the most energy-intensive, while titration, UV–Vis, and immunoassays (<0.1 kWh/sample) are the least. The final score is obtained by subtracting penalty points from 100, where a score between 50 and 75 indicates an acceptable level of greenness [42,43].

3. Results and Discussion

3.1. Implementation of AQbD approach.

3.1.1. ATP element.

For the HPTLC method, the ATP ensures accurate analyte quantification within a defined range and confidence level, while reliably detecting and measuring impurities within specified limits [30].

3.1.2. Risk assessment for the identification of CAAs and CMAs.

In this study, the retardation factor (R_f) was identified as the CAA, and the mobile phase composition (amounts of chloroform and methanol), chamber saturation time, and solvent front were considered as CMAs. A RAM was employed to identify and evaluate the CAAs and CMAs relevant to the HPTLC method. For systematic evaluation, all potentially significant CMAs were categorized and represented in a fishbone (Ishikawa) diagram (Figure 2). Based on this diagram, the most critical factors influencing the ATP were identified, and further risk assessment was performed using RAM. Parameters such as personnel, environmental factors (temperature, humidity), and instrument-related variables were maintained constant. Similarly, drying time and dye concentration (0.05% in ethanol: water, 80:20) were fixed to minimize variability. In the RAM, risk levels were categorized as high (+++), medium (++), and low (-) (Table 2). Low-risk factors had minimal influence on CAAs, medium-risk factors had a manageable yet noticeable effect, and high-risk factors significantly impacted CAAs, requiring stringent monitoring. Among the evaluated parameters, the mobile phase composition, mobile phase ratio, solvent front, and chamber saturation time exhibited a notable effect on the R_f value.

In summary, four CMAs—volume of methanol (A), volume of chloroform (B), chamber saturation time (C), and solvent front (D)—were considered for the proposed HPTLC method development, with the ATP defined as the R_f value of the drugs. For method optimization, a 2^{4-1} fractional factorial design (FFD) was employed to systematically analyze and optimize the relationship between CAAs and CMAs across three levels (-1, 0, +1).

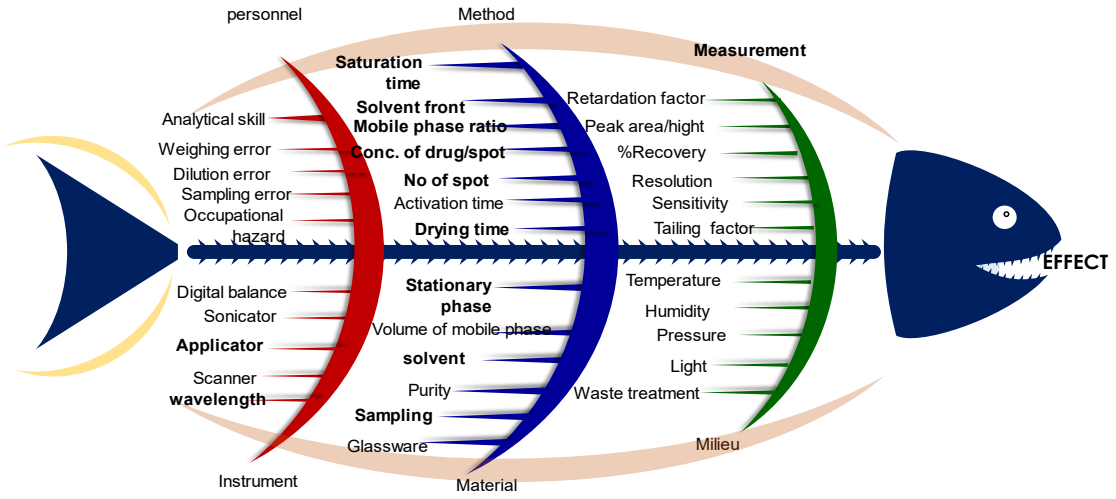

Figure 2. Ishikawa diagram.

Table 2. Risk assessment matrix.

CMA	CAA						
	Retardation factor	**Peak area**	**Peak hight**	**Resolution**	**%Recovery**	**Sensitivity**	**Tailing factor**
Mobile phase composition	+++	++	++	++	++	++	++
Mobile phase ratio	+++	++	++	++	++	++	++
Solvent front	+++	+	+	++	+	+	++
Chamber saturation time	+++	+	+	+	+	++	++
Wavelength	+	+	+	+	+	++	+
stationary phase (polar/non-polar)	++	+	+	++	+	+	+
No of spots on the plate	+	+	+	++	+	+	+
Volume of application	++	++	++	++	++	++	++

CMA	CAA						
	Retardation factor	**Peak area**	**Peak hight**	**Resolution**	**%Recovery**	**Sensitivity**	**Tailing factor**
concentration of drug/spot	+	++	++	++	++	++	++
Nature of solvent	++	+	++	++	+	+	++
Drying time	+	+	+	+	+	+	+

+++ = High level risk; ++ = Medium level risk; + = low level risk.

3.2. Development of HPTLC method.

Different solvent systems were used for mobile phase optimization, including methanol, chloroform, toluene, ethyl acetate, cyclohexane, n-hexane, acetone, IPA, diethyl ether, and acetonitrile, as shown in Table S1. To ensure accurate and repeatable separation of MH and GH, the mobile phase—Chloroform: Cyclohexane: Methanol: Ammonia (5:3:2:0.1 v/v/v/v)—was refined after numerous trials. Sharp, well-resolved peaks and respectable R_f values were obtained from chloroform, while cyclohexane balanced polarity and enhanced equilibrium. More environmentally friendly alternatives, such as acetone and ethyl acetate, did not perform as effectively. To eliminate the need for more harmful solvents, methanol, a greener solvent, was utilized. A small amount of ammonia also improved peak shape by reducing tailing. Overall, with minimal solvent usage and verified effectiveness, the approach maintains a commendable greenness profile. Despite the partial use of non-green solvents, the overall method exhibits a balanced greenness profile**.** The total volume of mobile phase used per analysis was minimal, and waste generation was significantly limited.

The sensitivity of the HPTLC method is dependent on the wavelength used. Detection wavelength for GH was 230 nm before derivatization, and for MH, 547 nm after derivatization with EY (Y) dye. A sharp and proportioned peak was produced by the mobile phase, composed of 'Chloroform: Cyclohexane: Methanol and Ammonia' (5: 3: 2: 0.2% v/v/v/v). As illustrated in Figure 3, GH and MH were identified at R_f 0.56 ± 0.04 (1000 ng/band) and R_f 0.28 ± 0.03 (1000 ng/band), respectively.

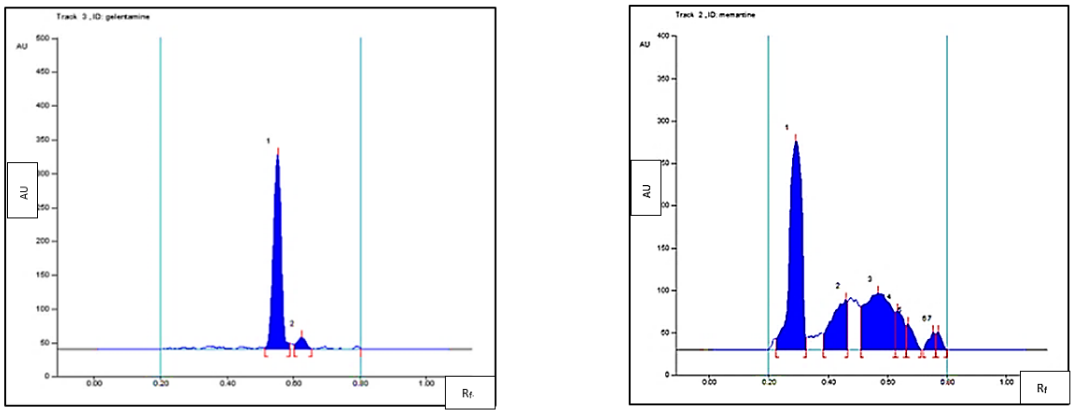

(a) **(b)**

Figure 3. TLC chromatogram of standard **(a)** GH*;* **(b)** MH.

3.3. Method validation.

3.3.1. Robustness.

DoE used to estimate the correlation between selected CMAs and CAA. Using a design matrix, a multivariate technique was used to examine simultaneous variation in the chosen

components with minor level deviations from the nominal value. All runs were independent and conducted in accordance with the design domain as indicated in Table 1, and robustness was assessed using FFD 2^{4-1}. The responses were observed and recorded. ANOVA and MLRA were applied to the results obtained from the study. Probability value (p-value), F value, and regression coefficient were calculated.

3.3.1.1. Effect on response Y_1.

A p-value of 0.05 or more is required for insignificant impacts. Model p-value for GH was observed as 0.1884, which means the method is robust enough, as shown in Table 3. The outcomes indicated that minor changes in CMAs did not significantly alter response (R_f value). In the case of GH, all factors were found to be insignificant. The model is not significant, as indicated by the GH model's Fisher (F) value of 16.13. The correlation coefficient value (R^2) was found to be 0.9988. S/N ratios greater than 4 are preferred, and the GH ratio of 10.58 indicated a strong enough signal. The modified R^2 values were high and closer to the expected values, signifying a significant correlation between the fitted models and the experimental data. Model repeatability was measured by the coefficient of variation (% CV), which was less than 10% (2.49 for GH). The polynomial equation 3 in terms of the coded factor for the response Y_1 can be used to forecast the response at a particular level.

$$Y1 = 0.567 + 0.020A + 0.025B - 0.007C + 0.032D - 0.007AB + 0.015AC \quad (3)$$

A positive value signifies a direct association between the independent and dependent factors. In this study, the volume of Methanol and chloroform in the mobile phase component and solvent front had a positive effect on the R_f value of drugs. It was seen from the polynomial equation that factor B (chloroform) had a greater coefficient value than factor A (methanol). Therefore, it may be said that the R_f value was influenced by the chloroform volume more. The solvent front also has a positive effect on R_f value because it acts as a reference point for calculating the distance traveled by the analyte, so as this distance increases, the R_f value of drugs also increases.

Table 3. ANOVA for response Y_1 and Y_2.

	Y_1			**Y_2**		
	Coefficient	**F value**	**P value**	**Coefficient**	**F value**	**P value**
Model	0.567	16.13	0.1884	0.306	170.33	0.0586
A	0.020	16.00	0.1560	0.021	289.00	0.0374
B	0.025	25.00	0.1257	0.023	361.00	0.0335
C	-0.007	2.25	0.3743	-0.011	81.00	0.0704
D	0.032	42.25	0.0972	0.016	169.00	0.0489
AB	-0.007	2.25	0.3743	-0.001	1.00	0.5000
AC	0.015	9.00	0.2048	0.013	121.00	0.0577
R^2 Value	0.9988			0.9990		
S/N ratio	10.58			35.52		

The Pareto chart is used to evaluate factor significance. Effects exceeding the Bonferroni limit are highly noteworthy, whereas those below the t-value threshold are likely insignificant. The importance of the variable crucial t-value at 0.05 was calculated to be 12,706 using a Pareto chart. Statistically non-significant variables were those whose absolute standard effect values fell below the crucial t-value. The Pareto chart, as shown in Figure 4a, demonstrated that among the four variables, none of them has a significant effect on the R_f value of GH. That means the GH R_f value was not that sensitive to changes in mobile phase composition and other CMAs.

To enhance comprehension of the outcomes, perturbation maps of the projected models are shown in Figure 4b. These graphs show how each element deviates from its designated reference value, leading to fluctuations in responses even when all other variables are held constant.

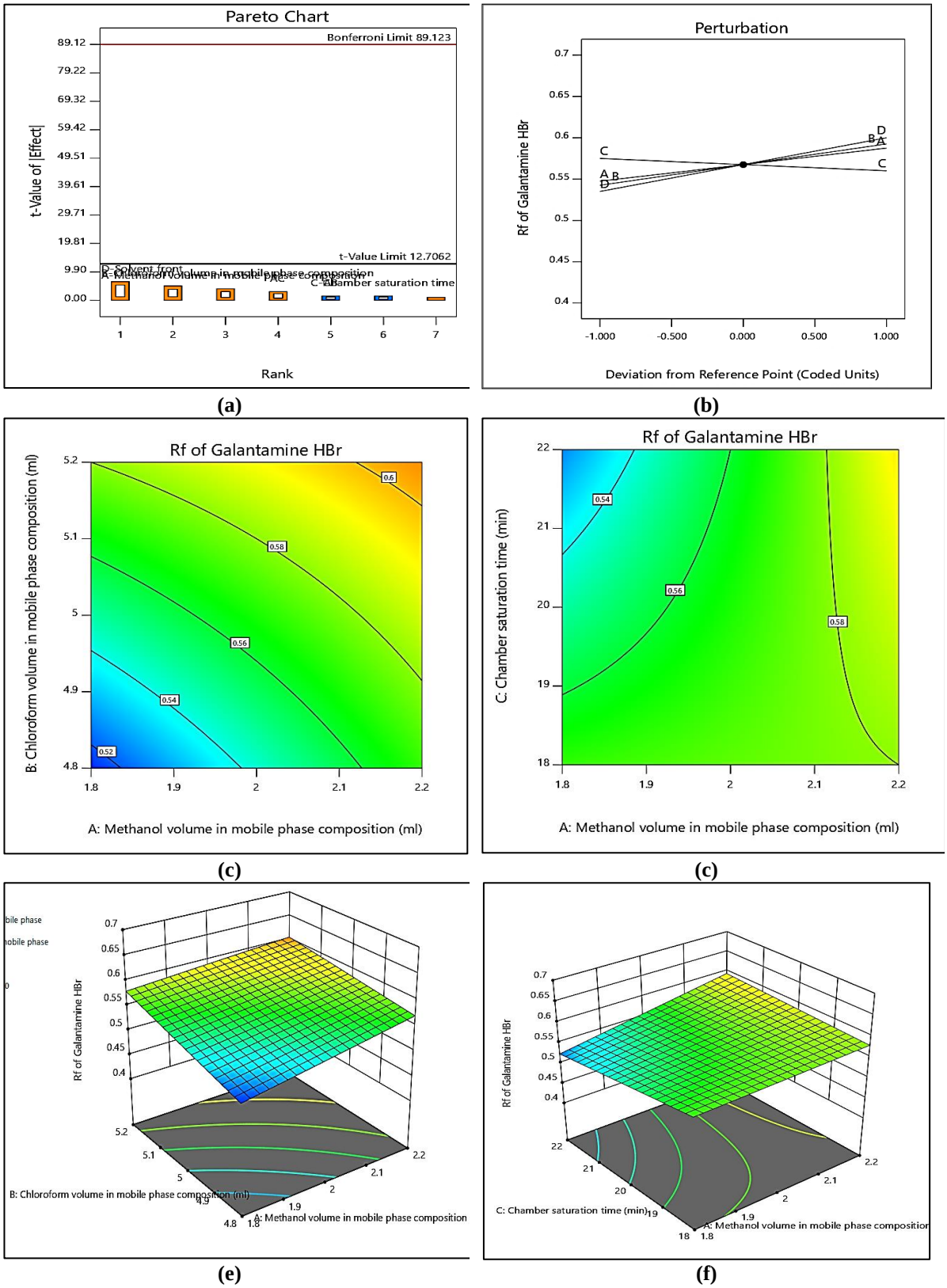

Figure 4. Effect of response Y_1 **(a)** Pareto chart; **(b)** perturbation plot; **(c)** Contour plot AB; **(d)** Contour plot AC; **(e)** 3D plot AB; **(f)** 3D plot AC on GH.

The most pronounced slope or curve denotes the sensitivity of the response to a particular stimulus. As each factor diverges from its definite standard value, the response changes, as seen in the graphs. The R_f value of the drug is most affected by any factor that deviates from the point. As can be seen from the graphs, factor c (chamber saturation time) has a greater impact on the R_f value of drugs than factors A, B, and D. The amount of methanol, chloroform, and solvent front in the mobile phase composition does not significantly alter the R_f value of drugs. However, because inadequate saturation can lead to irregular migration and uneven solvent distribution, even a small variation in the chamber saturation duration can significantly affect the R_f.

Analytical methodology creates three-dimensional response surface plots by varying two parameters while keeping the other two constant. If the regression model (e.g., a first-order model) includes only main effects without interactions, the response surface will be a plane with straight contour lines. In contrast, interactions in the model result in curved contour lines.

Figure 4 shows that when the volume of methanol and chloroform increases, the R_f value of GH increases somewhat. The reason is that as the amounts of methanol and chloroform increase, the mobile phase becomes increasingly polar, reducing the interaction between the stationary phase and the polar drugs. When a drug moves faster with the mobile phase, the R_f value increases. The R_f value increases with an increase in methanol volume (A) at constant chamber saturation time (C). Nevertheless, there is no statistical significance to this increase. The R_f value remains insignificant even with minute variations in the factor levels, demonstrating the robustness of the analytical method, as indicated by response surface analysis.

3.3.1.2. Effect on response Y_2.

The measured model p-value for MH was 0.0586, indicating that the technique is sufficiently robust, as shown in Table 3. Factors A, B, and D have a major impact on MH. The MH model's Fisher value (F) of 170.33 suggests that it is not significant. R^2 value was found to be 0.9990. An S/N ratio of more than four is ideal, and the ratio of 35.52 indicated a strong enough signal. Model repeatability is measured by the coefficient of variation (%CV), which is less than 10%. Here, the value found was 1.15 for MH. The polynomial equation 4, in terms of the coded factor, can be used to predict the response for a particular level, for both responses:

$$Y2 = 0.306 + 0.021A + 0.023B - 0.011C + 0.016D - 0.001AB + 0.013AC \quad (4)$$

A positive result indicates a direct link between the independent and dependent variables. Here, the R_f value of the drug was positively impacted by the quantity of methanol and chloroform in the mobile phase composition and the solvent front. Response is only slightly impacted by chamber saturation duration or interactions between methanol and chloroform. Factor B (chloroform) has a higher coefficient value than factor A (methanol), according to the polynomial equation. Thus, it could be said that the volume of chloroform had a prior effect on the R_f value of MH. Because the solvent front serves as a reference point for determining the distance traveled by the analyte, an increase in this distance also results in an increase in the R_f value of a drug.

The Pareto chart, as shown in Figure 5a, demonstrated that among the four variables, Chloroform and Methanol volume in the mobile phase composition and the solvent front had the greatest influence on the Rf of MH compared to GH, because MH has a stronger interaction

with the mobile phase composition than GH. So their R_f value was more sensitive to changes in the mobile phase component.

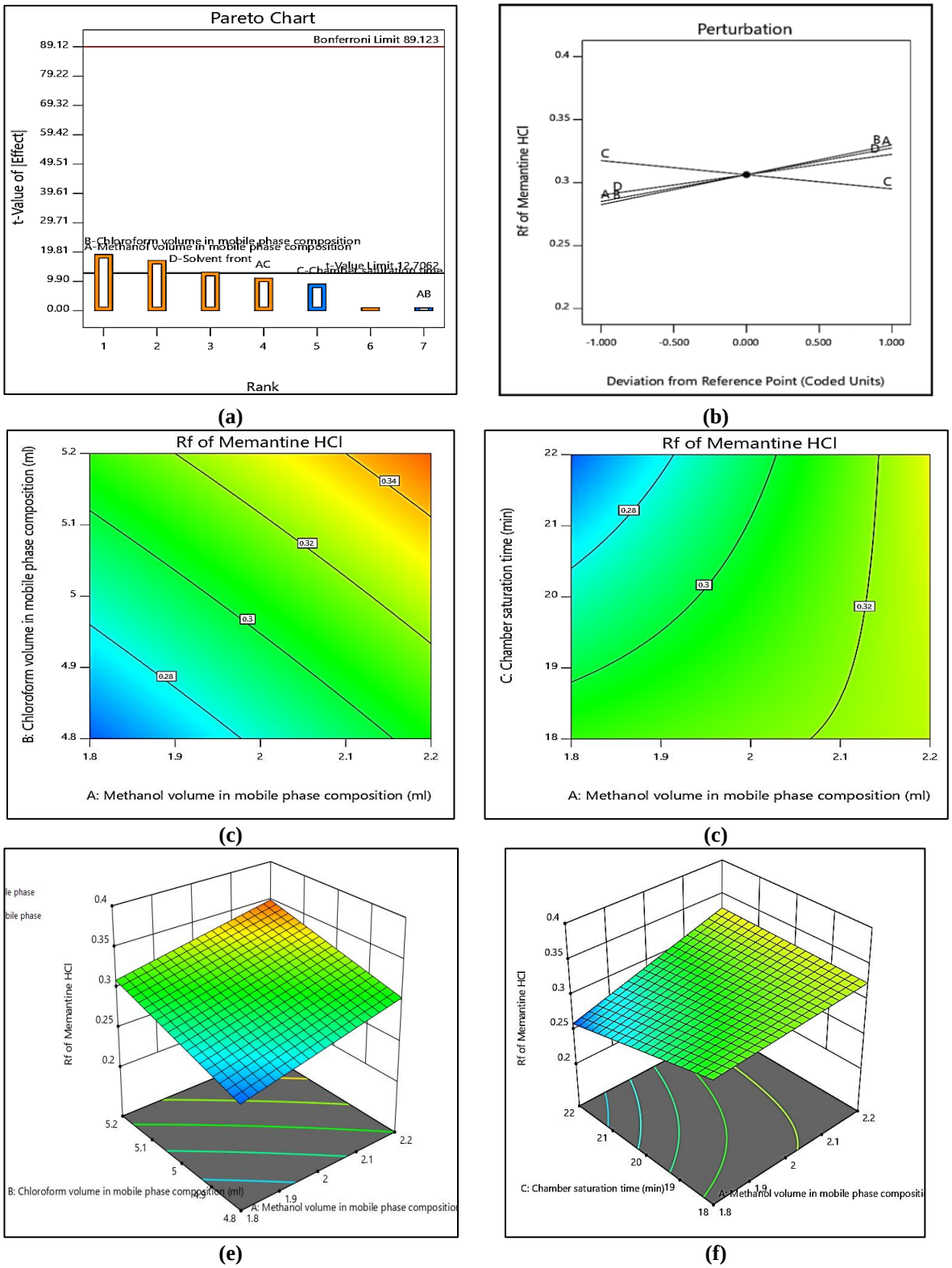

Figure 5. Effect of response Y2 **(a)** Pareto chart; **(b)** perturbation plot; **(c)** Contour plot AB; **(d)** Contour plot AC; **(e)** 3D plot AB; **(f)** 3D plot AC on GH.

According to perturbation plots shown in Figure 5b, the R_f value of the drug is most sensitive to chamber saturation time (C), and variations have a substantial effect on solvent migration and distribution. The methanol volume (A), the chloroform volume (B), and the solvent front (D) have little impact, on the other hand. Consistent outcomes depend on the chamber saturation time being optimized properly.

Figure 5 demonstrates that the MH R_f value rises as the volume of methanol and chloroform increases. The R_f is positively impacted by both parameters, with the greatest increase shown when A and C are both at higher values. This is because the mobile phase becomes more polar as the amounts of methanol and chloroform increase, thereby reducing the interaction between the polar drugs and the stationary phase. The R_f value increases as the drug moves more quickly with the mobile phase.

3.3.2. Standard curve of GH, MH, and linearity.

As shown in Figure 6 and Table S2-S3, the standard curve was created with peak area vs. concentration being linear for GH and MH in the 1500–4000 ng/band range. According to Table 4, the regression coefficient (R^2) values for GH and MH were 0.9969 and 0.9951, respectively, indicating that Beer's rule was followed.

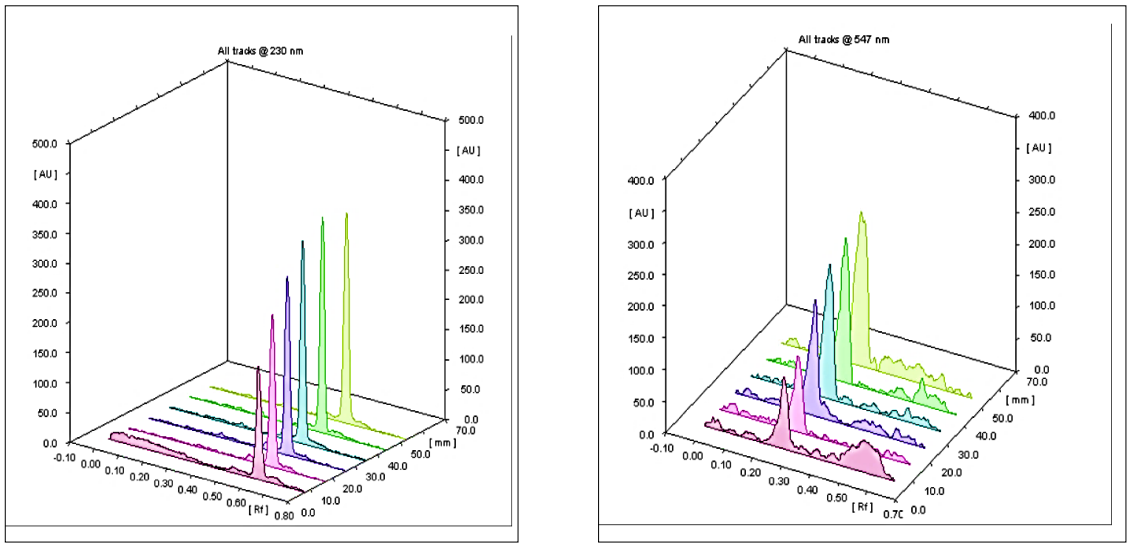

(a) **(b)**

Figure 6. Densitogram of **(a)** GH; **(b)** MH.

Table 4. HPTLC validation parameters.

Parameters	**MH**		**GH**	
Calibration limit [ng/ band]	1500-4000		1500-4000	
Regression equation	Y=1.8204X + 216.87		Y=1.9336X + 62.753	
R^2 value	0.9951		0.9969	
SD of slope	0.01		0.01	
SD of intercept	45.03		36.37	
LOD (ng/band)	88.25		63.36	
LOQ (ng/band)	267.44		192.02	
Precision (%RSD)				
Intra-day precision (%RSD)	0.41-0.68		0.35-0.54	
Inter-day precision (%RSD)	0.51-0.96		0.54-0.74	
Accuracy [%recovery ± %RSD]				
50%	100.72 ± 1.42		101.63 ± 1.13	
100%	99.51 ± 0.80		100.65 ± 0.95	
150%	101.84± 1.05		101.43± 1.43	
Specificity	**Developed Formulation**	**Standard**	**Developed Formulation**	**Standard**
r (S, M)	0.9965	0.9988	0.9998	0.9999
r (M, E)	0.9943	0.9983	0.9998	0.9999
R_f value	0.30	0.28	0.54	0.52
Analysis of SLAIF [%recovery ± %RSD]	**98.52±0.89**		**99.60±0.52**	

SD = standard deviation; %RSD = relative standard deviation.

3.3.3. LoD and LoQ.

The sensitivity of the developed method was demonstrated by measuring the LoQ and LoD for GH and MH. The LOD and LOQ values for GH were observed to be 63.36 and 192.02 ng/band, and for MH, they were 88.25 and 267.44 ng/band, respectively. The results indicated the high sensitivity of the developed method.

3.3.4. Precision.

To ascertain the precision of the developed approach, repeatability and intermediate precision were achieved. The precision was reported as the % RSD of peak area. %RSD < 2 indicated the appropriate precision in terms of sample application and peak area measurement repeatability.

3.3.5. Accuracy.

An accuracy study using the usual addition method revealed that the percentage recovery at each of the three levels ranged from 99.51 to 101.84%, indicating that the approach is appropriate and applicable for routine drug analysis, as displayed in Table 5 and Figure S2.

Table 5. Accuracy of GH and MH.

Drug	Recovery level (%)	Conc. of std spiked (ng/band)	Initial amount (ng/band)	Total concentration taken (ng/band)	Mean amount Found (ng/band)	% Recovery	SD	% RSD
GH	50	800	1600	2400	2416.05	101.63	1.14	1.13
	100	1600	1600	3200	3220.84	100.65	0.96	0.95
	150	2400	1600	4000	4057.38	101.43	1.45	1.43
MH	50	800	1600	2400	2417.28	100.72	1.20	1.18
	100	1600	1600	3200	3184.52	99.51	0.84	0.85
	150	2400	1600	4000	4073.77	101.84	1.09	1.07

3.3.6. Specificity.

For GH and MH, the generated overlaid spectra of the standard drugs and developed formulation displayed a peak at Retardation values of 0.56 for GH and 0.30 for MH, respectively, as shown in Figure 7.

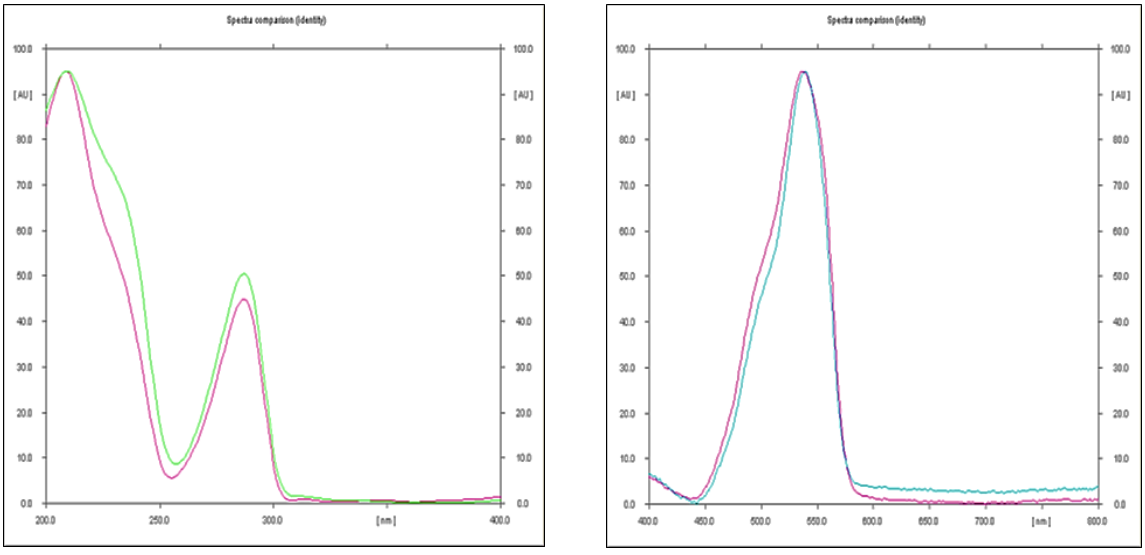

(a) **(b)**

Figure 7. Overlay spectra of standard and developed SLAIF showing peak purity of **(a)** GH*;* **(b)** MH.

The Rf values of the two drugs are identical. The purity of the active pharmaceutical ingredients in the developed formulation surpasses 0.99 for both peaks when the overlapping spectra at the 'highest', 'starting', and 'ending points' are compared to the standard.

3.3.7. Analysis of developed SLAIF.

A SLAIF containing 5 mg of GH and MH was analyzed, and the results showed an adequate recovery of both pharmaceuticals (99.6% for GH and 98.5% for MH) with % RSD less than 2% (n=3). This indicates that the approach can be used to regularly evaluate the quality of the pharmaceutical formulation.

3.4. Greenness appraisal.

Ten factors were considered to assess the applicability of BAGI: the type of analysis (single or multi), the analytical method, sample preparation, the reagents and materials used, the degree of automation, etc. These scores were used to create the score. A score of 80 on the BAGI, as seen in Figure 8a, indicates an exceptionally eco-friendly technique that is applicable and well-proportioned in terms of safety and environmental factors.

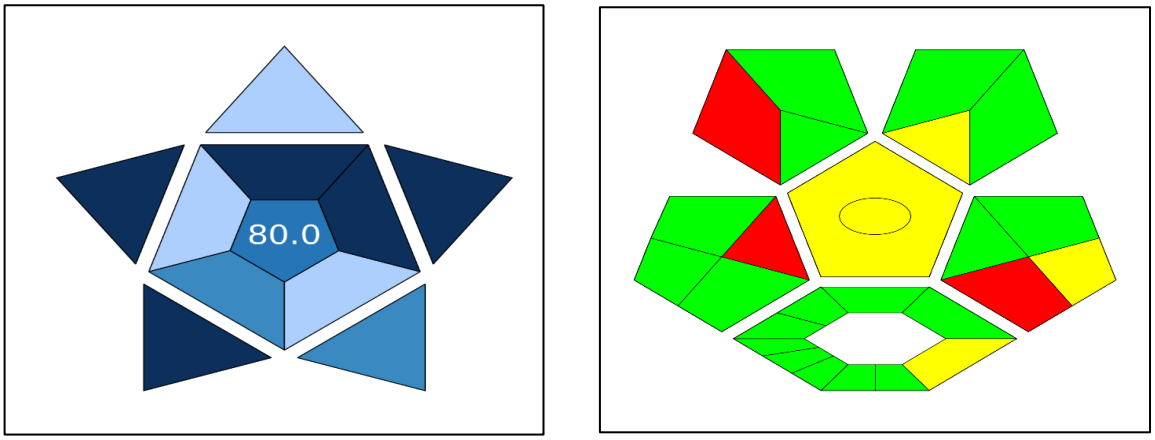

(a) **(b)**

Figure 8. (a) BAGI*;* **(b)** COMPLEX GAPI pictogram.

The COMPLEX GAPI is a tool that displays the results in a color-coded pictogram as shown in Figure 8 b. Sample preparation, reagents and solvent used, instrumentation, type of analysis, etc, based on these attributes, it evaluates greenness of the method.

Table 6. Analytical eco-scale greenness metric.

Items of the method	Value	Penalty points
Reagents		
Chloroform	<10 mL	1
Cyclohexane		1
Methanol		1
Instrument		
HPTLC	<0.1 kWh/sample	0
Hazard (physical, environmental, health)		
Reagent hazardous (Chloroform)	More severe hazard	4
Reagent hazardous (Methanol)	More severe Hazard	6
Reagent hazardous (cyclohexane)	More severe Hazard	8
Waste	>10mL	5
Total penalty points		26
Analytical eco scale score (HPTLC)		74

According to the color system, green is the most environmentally friendly color, yellow has a moderate effect, and red has a more negative effect. The pictogram shows mostly green and yellow signs, with fewer red signs for sample collection, solvents and reagents used, and waste treatment. The analytical eco scale uses a penalty-point system to evaluate greenness, and a score of 75 indicates an acceptable green method, as shown in Table 6.

4. Conclusion

An AQbD and DoE-based approach was used to develop a green, accurate, precise, and sensitive HPTLC method for the simultaneous estimation of Memantine HCl (MH) and Galantamine HBr (GH) in a smart long-acting injectable formulation. Critical parameters (ATP, CMAs, and CAAs) were identified through risk assessment using the Ishikawa diagram and RAM. A 2^{4-1} FFD optimized the chromatographic conditions, selecting chloroform:cyclohexane:methanol: ammonia as the mobile phase, with EY dye for MH detection. Well-resolved bands were obtained (Rf: 0.56 for GH, 0.28 for MH). Validation as per ICH Q2(R1) confirmed accuracy, precision, and robustness ($p > 0.05$). The Pareto chart showed that the solvent front and the volumes of chloroform and methanol in the mobile phase composition had the most significant effects on the Retardation value of MH compared to GH. The proposed analytical method was successfully applied to greenness appraisal using BAGI, COMPLEX GAPI, and analytical eco-scale tools, and was found to be greener. In future work, efforts will be made to explore greener solvent systems to enhance the method's environmental compatibility further, and in vivo evaluation will be required to confirm the method's applicability for routine bioanalysis and therapeutic monitoring.

Author Contributions

Conceptualization, P.R. and H.R.; methodology, P.R. and H.R.; software, P.R. and H.R.; validation, P.R. and H.R.; formal analysis, P.R. and H.R.; investigation, P.R. and H.R.; resources, P.R. and H.R.; data curation, P.R., H.R. and D.T.; writing—original draft preparation, P.R.; writing—review and editing, H.R., D.T. and V.T.; visualization, H.R.; supervision, H.R., D.T. and V.T.; project administration, P.R., H.R., D.T. and V.T.; funding acquisition, H.R., D.T. and V.T. All authors have read and agreed to the published version of the manuscript.

Institutional Review Board Statement

Not applicable.

Informed Consent Statement

Not applicable.

Data Availability Statement

Data sharing is not applicable.

Funding

This research received no external funding.

Acknowledgments

The authors would like to thank Anand Pharmacy College, Anand, Gujarat, India, for providing infrastructure support to do experimental work.

Conflicts of Interest

The authors declare no conflict of interest.

Abbreviations

The following abbreviations are used in this manuscript:

Abbreviation	Definition
AD	Alzheimer's Disease
NMDA	N-methyl D-aspartate
ACH	Acetylcholine
BAGI	Blue Applicability Grade Index
GAPI	Green Analytical Procedure Index
MH	Memantine HCl
GH	Galantamine HBr
AQbD	Analytical Quality by Design
ATP	Analytical Target Profile
CAA	Critical Analytical Attributes
CMA	Critical Method Attributes
EY dye	Eosin Y Dye
SLAIF	Smart Long- acting Injectable Formulation
FFD	Fractional Factorial Design
LoD	Limit of Detection
LoQ	Limit of Quantitation
PLGA	Polylactic Co-Glycolic Acid Polymer
GAC	Green Analytical Chemistry

References

1. Perumal, D.D.; Krishnan, M.; Lakshmi, K.S. Eco-friendly based stability-indicating RP-HPLC technique for the determination of escitalopram and etizolam by employing QbD approach. *Green Chem. Lett. Rev.* **2022**, *15*, 671-682, https://doi.org/10.1080/17518253.2022.2127334.
2. Manousi, N.; Wojnowski, W.; Płotka-Wasylka, J.; Samanidou, V. Blue applicability grade index (BAGI) and software:a new tool for the evaluation of method practicality. *Green Chem.* **2023**, *25*, 7598, https://doi.org/10.1039/D3GC02347H.
3. Monteiro, A.R.; Barbosa, D.J.; Remião, F.; Silva. R. Alzheimer's disease: Insights and new prospects in disease pathophysiology, biomarkers and disease-modifying drugs. *Biochem. Pharmacol*. **2023**, *211*, 115522, https://doi.org/10.1016/j.bcp.2023.115522.
4. Zhang, J.; Zhang, Y.; Wang, J.; Xia, Y.; Zhang, J.; Chen, L. Recent advances in Alzheimer's disease: Mechanisms, clinical trials and new drug development strategies. *Signal Transduct Target Ther.* **2024**, *9*, http://dx.doi.org/10.1038/s41392-024-01911-3.
5. Lee, J.; Varghese, M.; Meijer, E.; Langa, K.M.; Ganguli, M.; Angrisani, M. Prevalence of dementia in India : National and state estimates from a nationwide study. *Alzheimers Dement* **2023**, *19*, 2898-2912, https://doi.org/10.1002/alz.12928.
6. 2024 Alzheimer's association report disease facts and figures. *Alzheimers Dement* **2024**, *20*, 3708-3821, https://doi.org/10.1002/alz.13809.
7. Singh, B.; Day, C.M.; Abdella. S.; Garg, S. Alzheimer's disease current therapies, novel drug delivery systems and future directions for better disease management. *J. Control Release* **2024**, *367*, 402–24. https://doi.org/10.1016/j.jconrel.2024.01.047.
8. Breijyeh, Z.; Karaman, R. Comprehensive Review on Alzheimer's Disease: Causes and Treatment. *Molecules* **2020**, *25*, 5789, https://doi.org/10.3390/molecules25245789.

9. Tezel, G.; Ulutürk, S.; Reçber, T.; Timur, S.S.; Nemutlu, E.; Esendağlı, G. Preparation and in vitro characterization of memantine HCl loaded PLGA nanoparticles for Alzheimer's disease. *J Drug Deliv Sci Technol* **2024**, *100*, 106142, https://doi.org/10.1016/j.jddst.2024.106142.
10. Mahmoudi, M.; Saeidian, H.; Mirjafary, Z.; Mokhtari, J. Preparation and characterization of memantine loaded polycaprolactone nanocapsules for Alzheimer's disease. *J Porous Mater* **2021**, *28*, 205–12, https://doi.org/10.1007/s10934-020-00981-2.
11. Saleh, M.; Mohamed, J.M.M.; Ruby, J.J.; Kanthiah, S.; Alanazi, Y.F.; Majrashi, K.A. Preparation of Memantine-Loaded Chitosan Nanocrystals: In Vitro and Ex Vivo Toxicity Analysis. *Crystals* **2023**, *13*, 21, https://doi.org/10.3390/cryst13010021.
12. Du, L.; Liu, S.; Hao, G.; Zhang, L.; Zhou, M.; Bao, Y. Preparation and Release Profiles in Vitro/Vivo of Galantamine Pamoate Loaded Poly (Lactideco-Glycolide) (PLGA) Microspheres. *Front Pharmacol* **2021**, *11*, 619327, https://doi.org/10.3389/fphar.2020.619327.
13. Lohan, S.; Sharma, T.; Saini, S.; Swami, R.; Dhull, D.; Beg, S. QbD-steered development of mixed nanomicelles of galantamine: Demonstration of enhanced brain uptake, prolonged systemic retention and improved biopharmaceutical attributes. *Int. J. Pharm.* **2021**, *600*, 120482, https://doi.org/10.1016/j.ijpharm.2021.120482.
14. Sarfaraz, M.; Goel, T.; Doddayya, H. Formulation and Evaluation of Galantamine Hydrobromide Proniosome Gel for Alzheimer's disease. *J. Drug Deliv. Ther.* **2020**, *10*, 68–74.
15. Koola, M.M. Galantamine-Memantine combination in the treatment of Alzheimer's disease and beyond. *Psychiatry Res* **2020**, *293*, 113409, https://doi.org/10.1016/j.psychres.2020.113409.
16. Vishwas, S.; Awasthi, A.; Corrie, L.; Kumar Singh, S.; Gulati, M. Multiple target-based combination therapy of galantamine, memantine and lycopene for the possible treatment of Alzheimer's disease. *Med. Hypotheses* **2020**, *143*, 109879, https://doi.org/10.1016/j.mehy.2020.109879.
17. Koola, M.M.; Praharaj, S.K.; Pillai, A. Galantamine-memantine combination as an antioxidant treatment for schizophrenia. *Curr. Behav. Neurosci. Rep.* **2019**, *6*, 37-50, https://doi.org/10.1007/s40473-019-00174-5.
18. Dalwadi, S.; Thakkar, V.; Shah, P.; Patel, K. Optimizing Analysis of Donepezil HCl and Memantine HCl Using Multivariate Analysis as a Data Mining Tool in HPTLC Methodology. In Proceedings of the Human-Centric Smart Computing, Singapore, 2024//; Springer: Singapore, **2024**; Volume 376, pp. 309-321; https://doi.org/10.1007/978-981-99-7711-6_25.
19. Nunes, D.; Tavares, T.G.; Malcata, F.X.; Loureiro, J.A.; Pereira, M.C. Development and Validation of a Simple UV–HPLC Method to Quantify the Memantine Drug Used in Alzheimer's Treatment. *Pharmaceuticals* **2024**, *17*, 1162, https://doi.org/10.3390/ph17091162.
20. Taşpinar, N.; Bulduk, İ. Alternative Analytical Methods for Quantification of Galantamine in Pharmaceuticals. *Ege Tıp Bilim Derg* **2022**, *5*, 58–64, https://doi.org/10.33713/egetbd.1161168.
21. Kaur, A.; Nigam, K.; Srivastava, S.; Tyagi, A.; Dang, S. Memantine nanoemulsion: A new approach to treat Alzheimer's disease. *J Microencapsul* **2020**, *37*, 355–65, http://dx.doi.org/10.1080/02652048.2020.1756971.
22. Abou El-Alamin, M.M.; Toubar, S.S.; Mohamed, D.A.; Helmy, M.I. Development of Green HPTLC method for simultaneous determination of a promising combination Tamsulosin and Mirabegron: stability-indicating assay was examined. *BMC Chem.* **2023**, *17*, 1–18, https://doi.org/10.1186/s13065-023-01043-9.
23. Balekundri, A.; Hurkadale, P.J.; Hegde, H. Quality assessment, HPTLC-DPPH, Analytical Quality by Design based HPTLC method development for estimation of piperine in piper species and marketed formulations. *Green Anal Chem* **2024**, *8*, 100093, https://doi.org/10.1016/j.greeac.2024.100093.
24. Bodas, K.; Shinde, V.M.; Vishal, D.; Sheetal, D. Analytical Quality by Design (AQbD) Assisted Development and Validation of HPTLC Method for Estimation of Rottlerin in Topical Patch Formulation. *Pharmacognosy Res* **2023**, *15*, 267–76, https://doi.org/10.5530/pres.15.2.029.
25. Vanzara, R.; Bagada, H. Review on Implementation of AQbD Approach to the HPTLC method development and validation. *World journal of pharmaceutical research* **2023**, *12*, 1723–1741.
26. Shelke, P.G.; Chandewar, A.V. Validated stability-indicating high performance liquid chromatographic assay method for the determination of Dabigatran Etexilate Mesylate. *Res J Pharm Biol Chem Sci* ***2014***, *5*, 1637–44.
27. Amin, A.H.; Sheikh, R.El.; Fattah, G.M.A.; Ali, M.; Abdelnaby, B.M.; Gouda, A.A. Spectrophotometric Methods for the Quantitative Determination of Memantine Hydrochloride in Pure Form and

Pharmaceutical Formulations. *Int J Appl Pharm* **2022**, *14*, 206–14., https://dx.doi.org/10.22159/ijap.2022v14i2.43924.

28. Naffiz, S.; Ameena, S.; Eswarudu, M.; Babu, P.S.; Kumari, M.R.; Sindhuja, P.; Gouthami, P. Validated spectrophotometric methods for the determination of memantine hydrochloride in pure and tablet dosage form by using different chromogenic reagents. *World J. Pharm. Res* **2017**, *6*, 1198-1209.
29. Gaikwad, S.S.; Kalkate, S.D.; Bankar, A.A.; Bansode, A.S. Quality by design optimization and validation of a HPTLC-MS method for simultaneous estimation of paracetamol and prochlorperazine from bulk and formulation. *Int J Mass Spectrom* **2024**, *495*, 117171, https://doi.org/10.1016/j.ijms.2023.117171.
30. Martin, G.; Barnett, K.L.; Burgess, C.; Curry, P.D.; Ermer, J.; Gratzl, G.S. Lifecycle management of analytical procedures: Method development, procedure performance qualification, and procedure performance verification. *Pharmacopeial Forum* **2013**, *39*.
31. Nagar, P.; Garg, M.; Chauhan, C.; Kumar. R.; Chaudhary, A.K. Analytical Quality by Design (AQBD) Approach for HPLC Method Development, Method Optimization and Validation. *Int J Pharm Qual Assur* **2022**, 13,103–10.
32. Prajapati, P.; Gandhi, A.; Shah, S. Method Greenness Profile Assessment to AQbD-Driven Stability Indicating HPTLC Method for Estimation of Aripiprazole Using Screening Design and Response Surface Modeling. *J AOAC Int* **2023**, *106*, 501–13, https://doi.org/10.1093/jaoacint/qsac107.
33. Patel, M.M.R.; Patel, H.U. Analytical Quality by design (AQbD) approach : An advanced greener HPTLC method for Quantification of Lenvatinib in capsules. *African Journal of Biological Sciences* **2024**, *6*, 1603–16, https://doi.org/10.33472/AFJBS.6.Si2.2024.1603-1616.
34. Patel, K.G.; Shah, P.M.; Shah, P.A.; Gandhi, T.R. Validated high-performance thin-layer chromatographic (HPTLC) method for simultaneous determination of nadifloxacin, mometasone furoate, and miconazole nitrate cream using fractional factorial design. *J Food Drug Anal*. **2016**, *24*, 610–9, http://dx.doi.org/10.1016/j.jfda.2016.02.011.
35. Robert, M. Green Analytical Chemistry: A Sustainable Approach to Chemical Analysis. *Adv Appl Sci Res* **2023**, *14*, 107.
36. Pena-Pereira, F.; Tobiszewski, M.; Wojnowski, W.; Psillakis, E. A Tutorial on AGREEprep an Analytical Greenness Metric for Sample Preparation. *Adv. Sample Prep.* **2022**, *3*, 100025, https://doi.org/10.1016/j.sampre.2022.100025.
37. Albazi, S.; Al-Samarrai, E.T.; Alwan, L.H. Greenness appraisal and spectrophotometric estimation of carvedilol in pharmaceutical formulations and study kinetic parameters. *Green Anal. Chem.* **2024**, *11*, 100150, https://doi.org/10.1016/j.greeac.2024.100150.
38. Shah, M.; Patel, H.U.; Akabari, A.H. Eco-friendly HPTLC method for simultaneous estimation of gallic acid, ellagic acid, and curcumin biomarker in herbal formulation. *Essent Chem* **2024**, *1*, 1–10, https://doi.org/10.1080/28378083.2024.2420104.
39. AlSalem, H.S.; Algethami, F.K.; Magdy, M.A.; Ali, N.W.; Zaazaa, H.E.; Abdelkawy, M. High Performance Thin Layer Chromatography (HPTLC) Analysis of Anti-Asthmatic Combination Therapy in Pharmaceutical Formulation: Assessment of the Method's Greenness and Blueness. *Pharmaceuticals.* **2024**, *17*, 1–18, https://doi.org/10.3390/ph17081002.
40. Magdy, M.A.; Farid, N.F.; Anwar, B.H.; Abdelhamid, N.S. Four Greenness Evaluations of Two Chromatographic Methods : Application to Fluphenazine HCl and Nortriptyline HCl Pharmaceutical Combination in Presence of Their Potential Impurities Perphenazine and Dibenzosuberone. *Chromatographia* **2022**, *85*, 1075–86, https://doi.org/10.1007/s10337-022-04214-3.
41. Derayea, S.M.; Zaafan, A.A.S.; Nagy, D.M.; Oraby, M.; Amir, A.; Zaafan, S. Novel eco-friendly HPTLC method using dual-wavelength detection for simultaneous quantification of duloxetine and tadalafil with greenness evaluation and application in human plasma. *Sci. Rep.* **2024**, *14*, 23907, https://doi.org/10.1038/s41598-024-73523-4.
42. Hashmi, S.A.; Alegete, P. QbD green analytical procedure for the quantification of tolvaptan by utilizing stability indicating UHPLC method. *BMC Chem.* **2024**, *18*, 1–19, https://doi.org/10.1186/s13065-024-01214-2.
43. Foudah, A.I.; Shakeel, F.; Alqarni, M.H.; Alam P. A rapid and sensitive stability-indicating green RP-HPTLC method for the quantitation of flibanserin compared to green NP-HPTLC method: Validation studies and greenness assessment. *Microchem. J.* **2021**, *164*, 105960, https://doi.org/10.1016/j.microc.2021.105960.

Publisher's Note & Disclaimer

Supplementary materials

Table S1. Preliminary study for optimization of mobile phase.

Sr no.	Mobile phase composition	Eosin dye composition	Chamber saturation time	Rf of GH	Rf of MH	Inference
1.	Methanol: Toluene (7:3)	0.23% eosin dye in water	20 min	-	-	No peak found.
2.	n-Hexane: Ethyl acetate: Diethylamine (5:5:0.7)	Dragandoff reagent	25 min	0.11	-	Rf value of galantamine was found to be less & memantine peak was not found.
3.	Chloroform: Cyclohexane: Methanol (4:3:3)	0.2% eosin dye in water	20 min	0.61	0.58	Galantamine peak was merged & also area was less and improper memantine peak found
4.	Chloroform: Cyclohexane: Methanol (3:5:2)	0.5% eosin dye in water	20 min	0.45	0.23	Tailing occurs in the case of Galantamine & too many impurities were found in the Memantine peak.
5.	Chloroform: Cyclohexane: Methanol (4:4:2.5)	0.3% eosin dye in water	25 min	0.52	0.50	Improper shape of Galantamine was found & Memantine peak was broad & also impurities were more.
6.	Chloroform: Cyclohexane: Methanol (3:5:2)	0.3% eosin dye in water	20 min	0.44	0.23	Galantamine peak broadening occurred, and impurities were more present in case of Memantine
7.	Chloroform: Cyclohexane: Methanol (4:3:3)	0.1% eosin dye in Ethanol:Water 75:25)	20 min	0.64	0.48	Galantamine peak was merged with the solvent peak & area were less in the case of memantine peak. Impurities were reduced when using ethanol: water mixture.
8.	Chloroform: Cyclohexane: Methanol: Triethylamine (4:4:2:0.1)	0.1% eosin dye in Ethanol:Water 75:25	20 min	0.46	0.35	When TEA is used as a peak modifier for Galantamine peak was not merged, but the memantine peak was merged.
9.	Chloroform: Cyclohexane: Methanol: Triethylamine (4:3:2:0.1)	0.1% eosin dye in Ethanol:Water 80:20	20 min	0.60	0.39	Peak broadening occurs in Galantamine & Memantine peak.
10.	Chloroform: Cyclohexane: Methanol: Ammonia (4:4:2:0.1)	0.05% eosin dye in ethanol:water 80:20)	20 min	0.59	0.39	Ammonia was used as a peak modifier- so now Memantine peak was not merged, but Galantamine peak broadening was there.

Table S2. Linearity value of Galantamine HBr before derivatization.

Con. (ng/band)	Peak area ± SD
1500	3169.2±27.61
2000	3872.4± 29.72
2500	4807.8 ± 36.64
3000	5957.4 ± 35.02
3500	6616.4 ± 52.50
4000	7922.4 ± 55.39

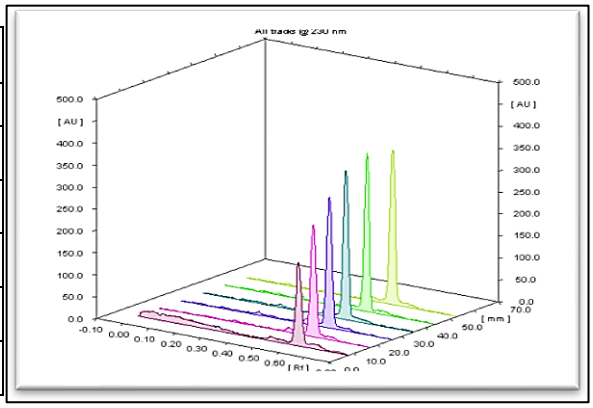

Table S3. Linearity value of Memantine HCl after derivatization.

Con. (ng/band)	Peak area ± SD
1500	3139.8±23.71
2000	3947.6± 21.03
2500	4814.2 ± 44.05
3000	5810.4 ± 39.86
3500	6598.6 ± 43.63
4000	7244.2 ± 45.50

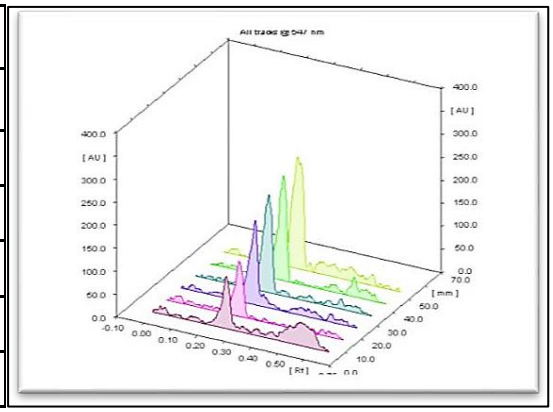

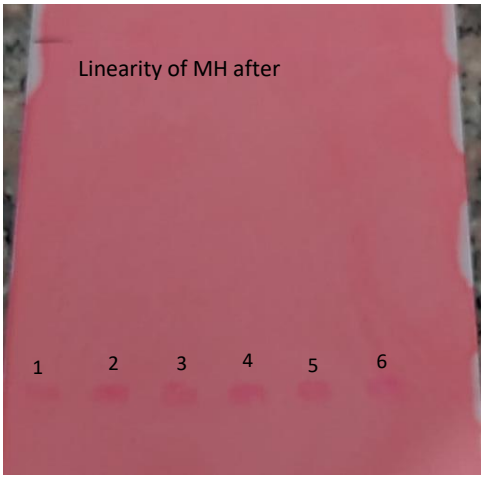

Figure S1. TLC plate after derivatization with eosin dye.

Table S4. Repeatability of GH.

Conc.(ng/band)	Area								
	1	2	3	4	5	6	Average Amplitude	SD	%RSD
2500	4834	4865	4787	4889	4875	4845	4849.167	36.37811	0.750193

Table S5. Intraday precision of GH.

Conc.(ng/band)	Area 1	Area 2	Area 3	Average Amplitude	SD	%RSD
2000	3862	3856	3823	3847	21	0.54588
3000	5981	5948	5932	5953.667	24.98666	0.419685
4000	7968	7914	7953	7945	27.87472	0.350846

Table S6. Interday precision of GH.

Conc.(ng/band)	Area	2	3	Average Amplitude	SD	%RSD
2000	3968	3924	3912	3934.667	29.48446	0.749351
3000	5856	5798	5849	5834.333	31.65965	0.542644
4000	7226	7315	7286	7275.667	45.39089	0.623873

Table S7. Repeatability of MH.

Conc. (ng/band)	1	2	3	4	5	6	Average Amplitude	SD	%RSD
2500	4865	4812	4798	4889	4875	4836	4845.8	36.36	0.750369

Table S8. Intraday precision of MH.

Conc.(ng/band)	Area 1	Area 2	Area 3	Average Amplitude	SD	%RSD
2000	3948	3912	3965	3941.667	27.06166	0.686554
3000	5838	5863	5887	5862.667	24.5017	0.417928
4000	7164	7189	7245	7199.333	41.4769	0.576121

Table S9. Interday precision of MH.

Conc.(ng/band)	Area	2	3	Average Amplitude	SD	%RSD
2000	3968	3896	3912	3925.333	37.80653	0.963142
3000	5856	5798	5842	5832	30.26549	0.518956
4000	7226	7315	7286	7275.667	45.39089	0.623873

Table S10. Accuracy of GH.

	% spike	Initial amt	Amt added	Total conc. of drug taken (ug/ml)	Total Conc. Of drug found (ug/ml)	% Recovery	Mean % Recovery	SD	% RSD
GH	50	1600	800	2400	2412.23	100.5096	101.6332	1.149353	1.130884
					2438	101.5833			
					2467.36	102.8067			
	100	1600	1600	3200	3250.541	101.5794	100.6515	0.963349	0.957114
					3223	100.7188			
					3189	99.65625			
	150	1600	2400	4000	4037.157	100.9289	101.4346	1.45498	1.434401
					4123	103.075			
					4012	100.3			

Table S11. Accuracy of MH.

	% spike	Initial amount	Amt added	Total conc. of drug taken (ug/ml)	Total Conc. Of the drug found (ug/ml)	% Recovery	Mean % Recovery	SD	% RSD
MH	50	1600	800	2400	2431.861	101.3276	100.72	1.433	1.42305
				2400	2378	99.08333			
				2400	2442	101.75			
	100	1600	1600	3200	3191.584	99.737	99.517	0.804	0.808157
					3156	98.625			

	% spike	Initial amount	Amt added	Total conc. of drug taken (ug/ml)	Total Conc. Of the drug found (ug/ml)	% Recovery	Mean % Recovery	SD	% RSD
					3206	100.1875			
	150	1600	2400	4000	4042.329	101.0582	101.84	1.079	1.059792
					4123	103.075			
					4056	101.4			

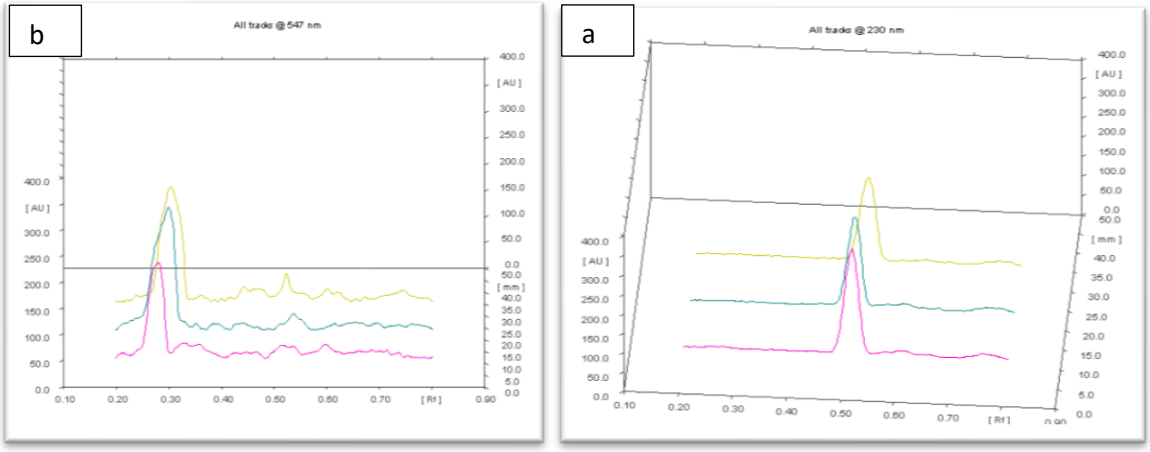

Figure S2. Accuracy of (a) GH & (b) MH.

Table S12. Specificity.

Correlation value	Standard		Developed formulation		Purity
	GH	MH	GH	MH	
r (S, M)	0.9999	0.9988	0.9998	0.9965	ok
r (M, E)	0.9999	0.9983	0.9998	0.9943	ok
R_f	0.52	0.28	0.54	0.30	-

Justification for mobile phase component selection

To ensure accurate and repeatable separation of memantine and galantamine, the mobile phase—Chloroform: Cyclohexane: Methanol: Ammonia (5:3:2:0.1 v/v/v/v)—was refined after numerous trials. Sharp, well-resolved peaks and respectable R_f values were obtained from chloroform, while cyclohexane balanced polarity and enhanced equilibrium. More environmentally friendly alternatives, such as acetone and ethyl acetate, did not perform as effectively. To eliminate the need for more harmful solvents, methanol, a greener solvent, was utilized. A small amount of ammonia also improved peak shape by reducing tailing. Overall, with minimal solvent usage and verified effectiveness, the approach maintains a commendable greenness profile. Despite the partial use of non-green solvents, the overall method exhibits a balanced greenness profile. The total volume of mobile phase used per analysis was minimal, and waste generation was significantly limited. In future work, efforts will be made to explore greener solvent systems to enhance the method's environmental compatibility further.